

Invited Paper

**REGULAR, CHAOTIC AND HYPERCHAOTIC VIBRATIONS
OF NONLINEAR SYSTEMS WITH SELF, PARAMETRIC
AND EXTERNAL EXCITATIONS**

UDC 534.14+534.141+516+93

Jerzy Warminski

Department of Applied Mechanics, Technical University of Lublin
Nadbystrzycka 36, 20-618 Lublin, Poland, e-mail: jwar@archimedes.pol.lublin.pl

Abstract. *Interactions between parametrically and self-excited vibrations for two models of self-excitation: van der Pol's and Rayleigh's, have been presented in this paper. It has been shown, that near the parametric resonance, the synchronisation phenomenon occurred, whereas out of those regions the system vibrated quasi-periodically. An additional external harmonic force has caused important changes in the resonance curve near the main parametric region. Moreover, for the large enough parametric excitation, the system has vibrated chaotically and hyperchaotically for the model with four potential "wells".*

1. INTRODUCTION

Mechanical vibrations which can appear in nature or in systems produced by a human being can be caused by different reasons. When a periodic external force acts on the mechanical system then we obtain vibrations called *forced vibrations*. A quite different class of vibrating systems are *self-excited* one. Their characteristic feature is, that a constant input can produce a periodic output. In this case, oscillations appear without depending on time excitations, but they are caused by internal properties of the system. *Parametric vibrations* are characterised by periodically in time changing parameters and they are described by homogeneous differential equations of motion. All above systems: self-, parametrically and externally excited are well known and deeply investigated in literature separately.

Paper [5] is one of the first works considering interactions between two different vibration types. There are only preliminary conclusions about interactions of parametric and self-excitations. More extensive research is presented e.g. in [1]. However, comprehensive and complex analysis is published in monograph [12] and paper [16].

They are devoted, as a whole, to the problem of parametrically and self-excited systems considering van der Pol's and Mathieu type models. There are numerical and analytical results obtained for different non-linear terms but mainly for one degree of freedom systems. Paper [7] presents interactions between parametrically and self-excited vibrations taking a non-symmetric quadratic elasticity characteristic into account. An additional external force influence acting on the parametrically and self-excited system with a frequency twice times smaller than the parametric excitation frequency is shown in [8], [9]. This additional force cases important differences in the main parametric resonance region. One of the newest and comprehensive researches considering interactions between parametric, external and self- excitations, as well as, for regular and chaotic motion is published in [13]. Important influence of an external harmonic force on the regular, chaotic and hyperchaotic motions is underlined in that monograph. New results for non-ideal systems are shown as well.

The main purpose of this work is to point out that interactions between different vibration types can lead to very complex behaviour, including chaotic motion, even for models with the simplest structure. Synchronisation areas of the system near the parametric resonance regions and transition paths from regular to chaotic motion are also presented. This paper has a review character and recapitulates same special results obtained by the author.

2. VIBRATING SYSTEM MODEL

Model of the parametric and self-excited system with many degrees of freedom can be described by the differential equations written in the matrix form

$$mx'' + f_d(x, x') + kx + f_p(x, \omega_p, t) + f_x(x) = \begin{cases} 0 \\ f_e(\omega, t) \end{cases} \quad (1)$$

where: x , x' , x'' - column matrixes of generalized co-ordinates, velocities and accelerations, respectively,

m , k - square, positive define matrixes of inertia and stiffness,

$f_d(x, x')$ - column matrix including functions of damping (self-excitation) of the system, $f_p(x, \omega_p, t)$ - column matrix including parametric excitations functions,

$f_x(x)$ - column matrix of non-linear stiffness functions,

$f_e(\omega, t)$ - external excitation column matrix.

2.1 MODEL WITH ONE DEGREE OF FREEDOM

At the beginning, the model of parametrically and self excited system with the simplest structure i.e. with one degree of freedom system is analysed. Fig.1 presents an oscillator consisting of a non-linear spring with symmetric Duffing's type stiffness and non-linear damping given by function $f(x, x')$, which represents a self-excitation of the system. The stiffness can change periodically and is assumed as Mathieu's type parametric excitation. Self-excitation is modelled by two of the often met in literature functions: van der Pol's and Rayleigh's.

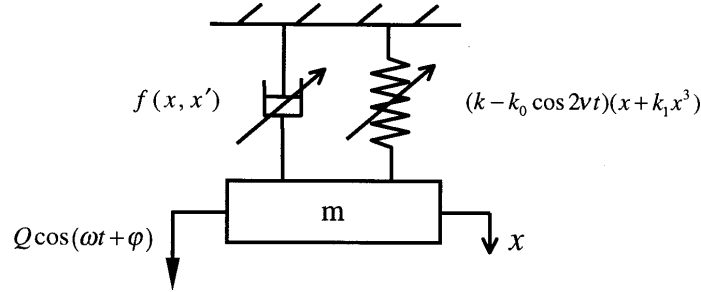


Fig. 1. Physical model of the system with one degree of freedom

Motion of the model in Fig.1 is described by a differential equation

$$mx'' + f(x, x') + (k - k_0 \cos 2\omega_p t)(x + k_1 x^3) = \begin{cases} 0 \\ Q \cos(\omega t + \varphi) \end{cases} \quad (2)$$

The dash means a derivative respect dimensional time, the function $f(x, x')$ represents self-excitation and is expressed as:

$$f_V(x, x') = (-c_1 + \hat{c}_1 x^2)x' \text{ for van der Pol's model, or}$$

$$f_R(x') = (-c_1 + \hat{c}_1 x'^2)x' \text{ for Rayleigh's model.}$$

The right side of Eq. (2) is considered in two variants, equal to zero i.e. without an external force influence or as a harmonic function.

Introducing dimensionless time $\tau = pt$ and a new dimensionless co-ordinate $X = x/x_{st}$, where: $p = \sqrt{k/m}$ is natural frequency of the system, $x_{st} = mg/k$ is its static displacement, the differential equation of motion is written in the dimensionless form

$$\ddot{X} + F_d(X, \dot{X}) + (1 - \mu \cos 2\vartheta\tau)(X + \gamma X^3) = \begin{cases} 0 \\ q \cos(\Omega\tau + \varphi) \end{cases} \quad (3)$$

The dimensionless parameters in Eq. (3) are defined as:

$$\alpha = \frac{c_1}{mp}, \quad \beta = \frac{c_2 p}{m} x_{st}^2, \quad \gamma = k_1 x_{st}^2, \quad \mu = \frac{k_0}{k}, \quad q = \frac{Q}{mx_{st}}, \quad \vartheta = \frac{\omega_p}{p}, \quad \Omega = \frac{\omega}{p}, \quad \dot{X} = \frac{dX}{d\tau},$$

$$\ddot{X} = \frac{d^2 X}{d\tau^2}, \quad F_d(X, \dot{X}) = F_V(X, \dot{X}) = (-\alpha + \beta X^2)\dot{X} \text{ - for van der Pol's model and}$$

$$F_d(X, \dot{X}) = F_R(X, \dot{X}) = (-\alpha + \beta \dot{X}^2)\dot{X} \text{ - for Rayleigh's model.}$$

Assuming that the system is weakly non linear, all non-linear terms are collected on the right side of the Eq. (3) and the parameters are expressed by a formal small parameter ε .

$$\ddot{X} + X = \varepsilon \{ \tilde{F}(X, \dot{X}) + \tilde{\mu} \cos 2\vartheta\tau X - \tilde{\gamma} X^3 + \varepsilon \tilde{\gamma} \tilde{\mu} X^3 \cos 2\vartheta\tau + \tilde{q} \cos(\Omega\tau + \varphi) \} \quad (4)$$

where: $\alpha = \varepsilon \tilde{\alpha}$, $\beta = \varepsilon \tilde{\beta}$, $\gamma = \varepsilon \tilde{\gamma}$, $\mu = \varepsilon \tilde{\mu}$ are small and positive.

It is worth to underline that the term $\varepsilon \tilde{\gamma} \tilde{\mu} X^3 \cos 2\vartheta\tau$ in Eq. (4) appears in the second order perturbation. If this term is equal to zero the parametric excitation is called linear, otherwise the parametric excitation is coupled with non-linear terms and then it is called non-linear parametric excitation [12].

2.2 ANALYTICAL INVESTIGATIONS

Due to the non-linearity of the considered system, the differential equation of motion (4) is solved by applying an approximate analytical method. The solution is found by using multiple scale of time method near the parametric resonances [6].

Let us assume that the parameter ε is small and positive. Next, we introduce different time scale $T_0 = \tau$, $T_1 = \varepsilon\tau$, $T_2 = \varepsilon^2\tau$, ..., where T_0 is a fast scale and T_1, T_2, \dots are slower time scale, which characterize the phase and the amplitude modulations, caused by the system non-linearity. In general for n scale of time we can write

$$T_n = \varepsilon^n \tau \quad (5)$$

The approximate solution of Eq. (4) is assumed as a small parameter series

$$X(\tau, \varepsilon) = X_0(T_0, T_1, T_2) + \varepsilon X_1(T_0, T_1, T_2) + \varepsilon^2 X_2(T_0, T_1, T_2) + \dots \quad (6)$$

In this method time derivatives take new definitions:

$$\frac{d}{d\tau} = D_0 + \varepsilon D_1 + \varepsilon^2 D_2 + \dots, \quad \frac{d^2}{d\tau^2} = D_0^2 + 2\varepsilon D_0 D_1 + \varepsilon^2 (2D_0 D_2 + D_1^2) + \dots$$

Notation $D_n^m = \frac{\partial^m}{\partial T_n^m}$ means m order derivative respect n time scale.

When excitation frequency ϑ and the natural frequency p satisfies relationship $m\vartheta = np$, where m, n are natural numbers then the system vibrates near the resonance area. Because the natural frequency of the considered system $p = 1$, therefore we can write

$$\frac{m^2}{n^2} \vartheta^2 = 1 + \varepsilon \sigma_1 \quad (7)$$

where, σ_1 is detuning parameter.

Introducing the solution (6) into Eq. (4), taking new definitions of the first and second derivatives and grouping terms of the same order ε , we obtain recurrent differential equations in consecutive perturbation orders:

- ε^0 order approximation

$$D_0^2 X_0 + \frac{m^2}{n^2} \vartheta^2 X_0 = 0 \quad (8)$$

- ϵ^1 order approximation

$$D_0^2 X_1 + \frac{m^2}{n^2} \vartheta^2 X_1 = \sigma_1 X_0 - 2D_0 D_1 X_0 + \tilde{F}_{d0} - \tilde{\gamma} X_0^3 + \tilde{\mu} X_0 \cos 2\vartheta\tau + \tilde{q} \cos(\Omega\tau + \varphi) \quad (9)$$

- ϵ^2 order approximation

$$D_0^2 X_2 + \frac{m^2}{n^2} \vartheta^2 X_2 = \sigma_1 X_1 - D_1^2 X_0 - 2D_0 D_1 X_1 - 2D_0 D_2 X_0 + \tilde{F}_{d1} - 3\tilde{\gamma} X_0^2 X_1 + \tilde{\mu} X_1 \cos 2\vartheta\tau + \tilde{\gamma}\tilde{\mu} X_0 \cos 2\vartheta\tau \quad (10)$$

where \tilde{F}_{d0} and \tilde{F}_{d1} are damping terms taking forms respectively

- for Rayleigh's model

$$\tilde{F}_{d0} = \tilde{\alpha} D_0 X_0 - \tilde{\beta} D_0 X_0^3, \quad \tilde{F}_{d1} = \tilde{\alpha}(D_0 X_1 + D_1 X_0) - 3\tilde{\beta}(D_0 X_0^2 D_0 X_1 - D_0 X_0^2 D_1 X_0)$$

- for van der Pol's model

$$\tilde{F}_{d0} = \tilde{\alpha} D_0 X_0 - \tilde{\beta} D_0 X_0 X_0^2, \quad \tilde{F}_{d1} = \tilde{\alpha}(D_0 X_1 + D_1 X_0) - \tilde{\beta}(X_0^2 D_0 X_1 - X_0^2 D_1 X_0 + 2X_0 X_1 D_0 X_0)$$

Solution of the Eq. (8) has form

$$X_0(T_1, T_2, T_3) = A(T_1, T_2) \exp\left(i \frac{m}{n} \vartheta T_0\right) + \bar{A}(T_1, T_2) \exp\left(-i \frac{m}{n} \vartheta T_0\right) \quad (11)$$

and function $A(T_1, T_2)$ can be expressed as

$$A = \frac{1}{2} a \exp(i\Phi) \quad (12)$$

where: a and Φ are vibrations amplitude and phase, respectively, and $i = \sqrt{-1}$. Solving successively the differential equations system (8)-(10) we can obtain the approximate solution for generalized co-ordinate, whereas the amplitude and phase modulation equations are found from the secular term elimination conditions.

In this paper, only the most important resonance area i.e. the main parametric resonance is taken into account. Analysis of secondary type resonances is presented in [13]. To get solutions in the neighborhood of the main parametric resonance around $\vartheta \approx 1.0$, it is necessary to substitute in (7)-(10) the natural numbers $m=n=l$. At the beginning we take $q=0$ and then the external harmonic force is neglected. The approximate solution for these assumption has form

$$X = a \cos(\vartheta\tau + \Phi) + \epsilon \left[\frac{1}{32\vartheta^2} \tilde{\gamma} a^3 \cos(3\vartheta\tau + 3\Phi) - \frac{1}{16\vartheta^2} \tilde{\mu} a \cos(3\vartheta\tau + \Phi) + \tilde{C} \sin(3\vartheta\tau + 3\Phi) \right] \quad (13)$$

and modulation equations of the amplitude and the phase in the second order approximation are

$$\dot{a} = \tilde{W}_1 + \frac{1}{4\vartheta} \epsilon \tilde{\mu} a \left(1 + \frac{5}{16\vartheta^2} \epsilon \tilde{\gamma} a^2 - \frac{1}{2} \epsilon \tilde{\gamma} a^2 \right) \sin 2\Phi \quad (14)$$

$$\begin{aligned}
a\dot{\Phi} = \tilde{W}_2 - a & \left(\frac{1}{2\vartheta}(-1+\vartheta^2) + \frac{1}{8\vartheta^3}(-1+\vartheta^2)^2 - \frac{3}{64\vartheta^3}\varepsilon^2\tilde{\mu}^2 \right) \\
& + a^3 \left(\frac{3}{8\vartheta}\varepsilon\tilde{\gamma} + \frac{3}{16\vartheta^3}\varepsilon\tilde{\gamma}(-1+\vartheta^2) \right) - \frac{15}{256\vartheta^3}\varepsilon^2\tilde{\gamma}^2 a^5 \\
& - \frac{1}{4\vartheta} \left(\varepsilon\tilde{\mu} + \left(\frac{1}{8\vartheta^2} + 1 \right) \varepsilon^2\tilde{\gamma}\tilde{\mu}a^2 \right) a \cos 2\Phi
\end{aligned} \tag{15}$$

Parameters used in Eqs. (13)-(15) are defined as

– for Rayleigh's model

$$\tilde{C}_R = \frac{1}{32}\tilde{\beta}\vartheta a^3,$$

$$\tilde{W}_{1R} = \frac{1}{2}\varepsilon\tilde{\alpha}a - \frac{3}{16\vartheta^2}\varepsilon^2\tilde{\alpha}\tilde{\gamma}a^3 - \frac{3}{8}\varepsilon\tilde{\beta}a^3 - \frac{3}{32}\varepsilon^2\tilde{\beta}\tilde{\gamma}a^5 + \frac{7}{64}\varepsilon^2\tilde{\beta}\tilde{\mu}a^3 \cos(2\Phi)$$

$$\tilde{W}_{2R} = -\frac{1}{8\vartheta}\varepsilon^2\tilde{\alpha}^2 a + \frac{9}{256}\varepsilon^2\tilde{\beta}^2\vartheta^3 a^5$$

– for van der Pol's model

$$\tilde{C}_V = -\frac{1}{32\vartheta}\tilde{\beta}a^3,$$

$$\tilde{W}_{1V} = \frac{1}{2}\varepsilon\tilde{\alpha}a - \frac{3}{16\vartheta^2}\varepsilon^2\tilde{\alpha}\tilde{\gamma}a^3 - \frac{1}{8}\varepsilon\tilde{\beta}a^3 + \frac{1}{32\vartheta^2}\varepsilon^2\tilde{\beta}\tilde{\gamma}a^5 + \frac{1}{64\vartheta^2}\varepsilon^2\tilde{\beta}\tilde{\mu}a^3 \cos(2\Phi),$$

$$\tilde{W}_{2V} = -\frac{1}{8\vartheta}\varepsilon^2\tilde{\alpha}^2 a + \frac{1}{8\vartheta}\varepsilon^2\tilde{\alpha}\tilde{\beta}a^3 - \frac{7}{256\vartheta}\varepsilon^2\tilde{\beta}^2 a^5 - \frac{1}{32\vartheta^2}\varepsilon^2\tilde{\mu}\tilde{\beta}a^3 \sin(2\Phi)$$

Equations (14) and (15) let us to determine the amplitude and the phase in the steady state by assuming $\dot{a} = 0$, $\dot{\Phi} = 0$.

2.3. REGULAR VIBRATIONS

Exemplary calculations for one degree of freedom system are performed basing on the formulae derived in the former chapter. Calculations are done for parameters as in papers [8], [9], [13].

$$\alpha = 0.01, \quad \beta = 0.05, \quad \gamma = 0.1, \quad \mu = 0.2, \quad q = 0$$

The vibration amplitudes found for two types of self-excitations, van der Pol's and Rayleigh's are presented in Fig.2a and Fig.2b, respectively. These results are obtained by solving equations (14) and (15) in the steady state. Parameter $q=0$, what means that there is not an external force in the system and the right side of Eq. (3) is equal to 0.

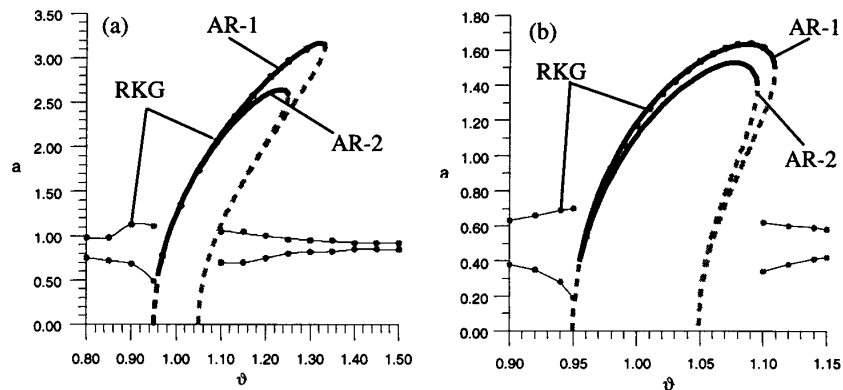


Fig. 2. Vibration amplitudes in the main parametric resonance neighbourhood, (a) van der Pol's model, (b) Rayleigh's model, AR-1, AR-2 –non-linear and linear parametric excitations, RKG-numerical simulation

Index AR-1 marks amplitudes for the non-linear parametric excitation, whereas AR-2 corresponds to the linear one. To verify analytical solutions, the numerical simulation results obtained by fourth order Runge-Kutta-Gill's method are marked in the figures (RKG). In the neighborhood of the main parametric resonance self-excited vibrations are pulled in by the parametric excitation and the synchronization phenomenon is observed (solid line in Fig. 2). The system vibrates with a constant amplitude and a single frequency. Outside the synchronization area, the system vibrates quasi-periodically, and the motion is composed by two vibrations having incommensurable frequencies, self- and parametric excitations. As a result of this interaction, outside the resonance region, the amplitude modulations are observed. On the Poincaré section, they are represented by stable and unstable quasi-periodic limit cycles [16]. An envelope of the modulated amplitude in Fig. 2 is marked by two points, the upper point corresponds to the maximal amplitude value, the lower one to the minimal modulation value. Resonant curves presented in Fig. 2 have similar qualitative properties, as well as for van der Pol's, as for Rayleigh's damping models. Only a quantitative difference takes place.

One of the most important tasks, from practical point of view, is to determine the synchronization area width and the system parameters influence on the vibrations amplitudes. The synchronization area begins in the point, in which the non-trivial and stable solutions appear.

It corresponds to the resonance curve stable part beginning. As follows from the analytical research, if $\tilde{\mu} < \tilde{\alpha}\sqrt{4 - \varepsilon^2\tilde{\alpha}^2}$, then the resonance curve has a closed shape, and don't have joint points with ϑ axis. In Fig. 3, the plane α - μ is divided on two parts, the dark area corresponds to parameters α , μ , where the bifurcation points trivial into non-trivial solutions does not exist. In a small range of parameters α and μ , the limit

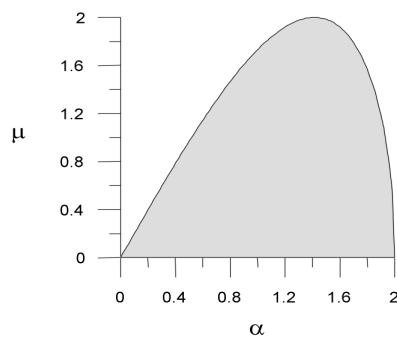


Fig. 3. Bifurcation regions of trivial into nontrivial solutions

is determined by a slope of a straight line $\mu/\alpha \approx 2$. Thus, for small parameters value, the condition of the non-trivial solutions occurring can be written as

$$\frac{\mu}{\alpha} > \sim 2 \quad (16)$$

This inequality sets the relation between parametric (μ) and self- (α) excitations, which has to be satisfied to obtain non-trivial solutions (synchronisation area). If this ratio (16) is bigger, then the synchronisation area is wider and the synchronized amplitudes are larger. Vibrations time histories and their power spectra before, inside and after synchronisation area are presented in Fig. 4. Before the synchronisation the system vibrates quasi-periodically (Fig. 4.a,b), next the synchronisation effect takes place (Fig. 4.c,d) and after getting out of the synchronisation region the quasi-periodic motion occurs again. One can notice that the small peak in power spectra figures changes its position respect the system natural frequency.

Synchronisation regions are well visible in bifurcation diagrams presented in Fig. 5. Three synchronisation regions are mapped by a line. Number 2 marks the main parametric resonance, number 1 the fundamental parametric resonance and number 3 secondary parametric resonance [13], [14]. Dark areas correspond to quasi-periodic motion.

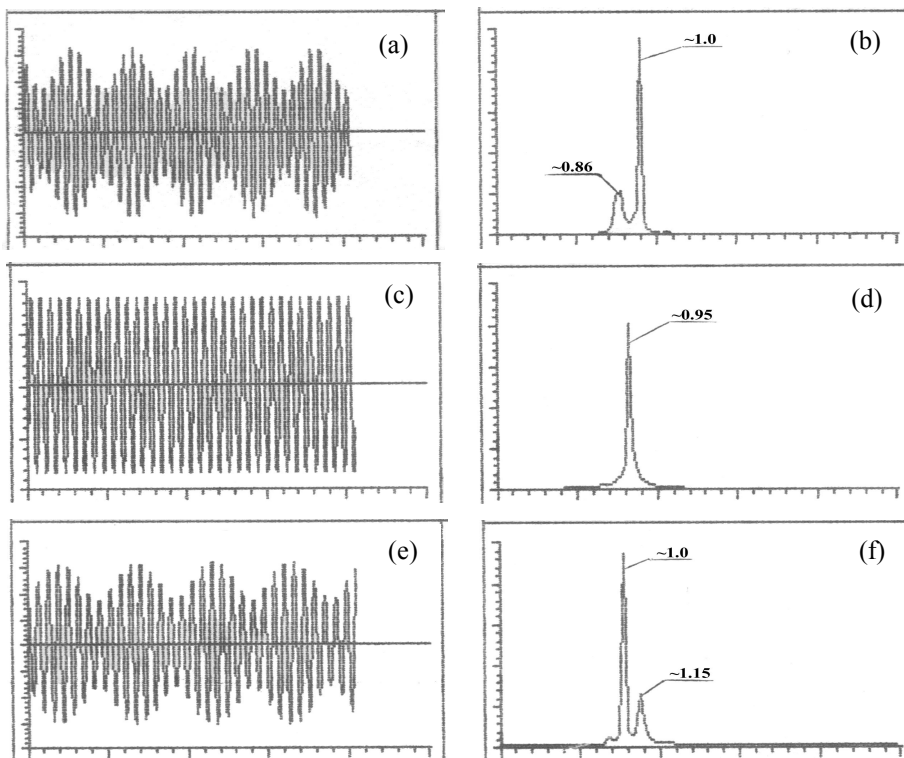


Fig. 4. Transition through the main parametric resonance, time histories and power spectra for $\vartheta = 0.92$ (a),(b); $\vartheta = 0.95$ (c),(d); $\vartheta = 1.1$ (e),(f)

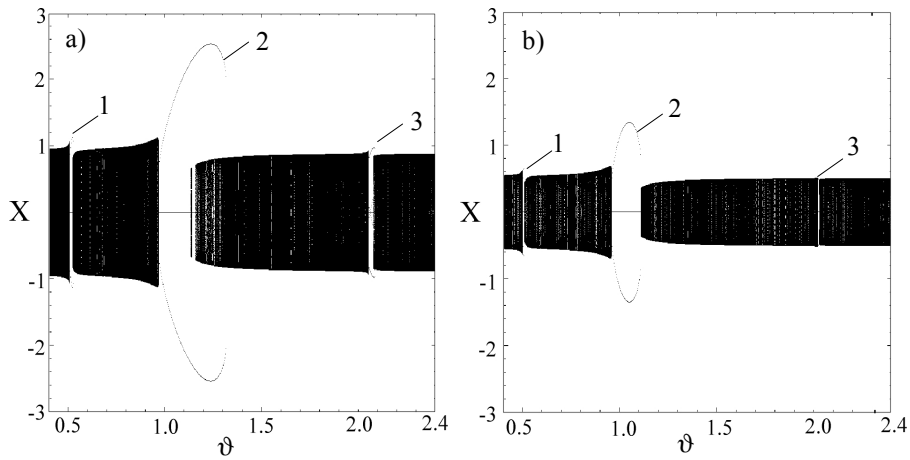


Fig. 5. Bifurcations diagrams, (a) van der Pol's model; (b) Rayleigh's model

The biggest synchronisation region appears near the main parametric resonance (No. 2 in Fig. 5). Bifurcation diagrams confirm that for both models of self-excitations results are in qualitative agreement. Only quantitative differences appear, but the character of motion is similar.

Let consider dynamics of the parametrically and self-excited system under an additional external harmonic force influence, now $q \neq 0$. In such a case, three different types of excitation can interact: self, parametric and external one.

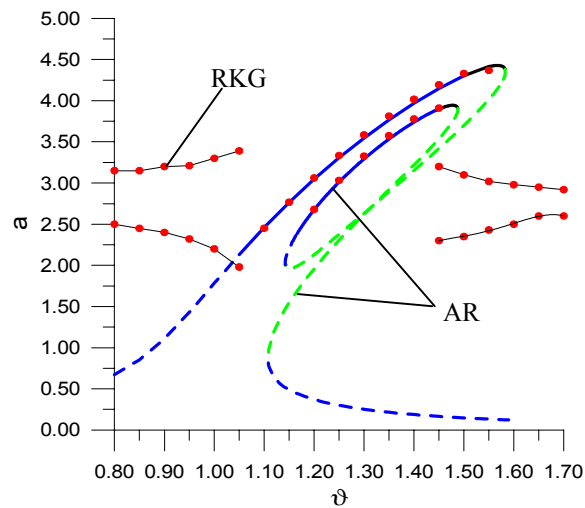


Fig. 6. Synchronisation area in the main parametric resonance neighbourhood with external force influence, van der Pol's model, $q=0.2$, $\alpha=0.1$

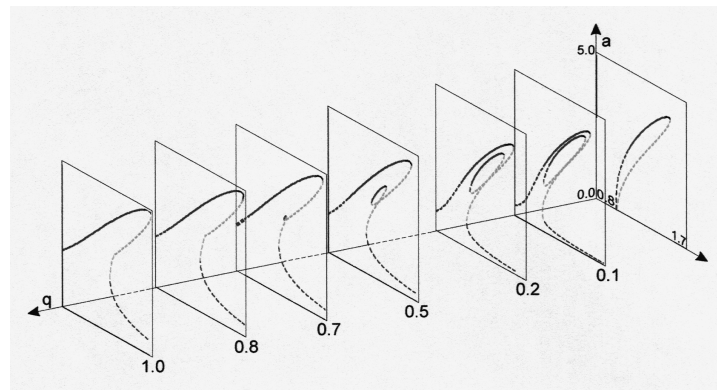


Fig. 7. Synchronisation areas near the main parametric resonance for different external force amplitudes, $q=0; 0.1; 0.2; 0.5; 0.7; 0.8; 1.0$; van der Pol's model, $\alpha=0.1$

Let us assume that the external force frequency is ϑ while the parametric excitation's is $2J$ and both have the same phase. In Eq. (4) we substitute $W=J, j=0$. It means that the system is forced additionally near the main parametric resonance. Solutions for this case are found basing on the analytical results [8], [9], [14]. Fig. 6 presents an amplitude - frequency characteristic assuming small value of external force $q=0$. We can observe (Fig. 6) that the additional force changes radically the shape of the resonance curve. Additional solutions, visible as an internal loop, appear inside the synchronisation region. Their stability analysis reveals that only upper part of the loop is stable. The lower part is unstable. This result means that for one assumed excitation frequency even five solutions are possible, however only two upper are stable. Further analysis shows that this new effect is possible only for small values of the external force. If the amplitude of external force increases then character of the resonance curve changes gradually and the curve has a classical shape. This transition is presented in Fig. 7. Similar results, as well for van der Pol's, as for Rayleigh's models are obtained.

2.5 TRANSITION TO CHAOTIC VIBRATIONS

The parametric excitation μ is one of the most important bifurcation parameters of the considered dynamical system. Therefore, analysis of this parameter influence on the parametric and self- excited system is investigated in this chapter.

To comparing results of both damping models it is assumed that parameter β in Rayleigh's model is three times smaller than for van der Pol's one, $\beta = 0.05/3 \approx 0.0166$. Such parameter value enables two damping models comparison. The first dark area, appearing in both figures for small parameter μ , represents quasi-periodic motion. For $\mu \approx 0.08$ the inverse *secondary Hopf's bifurcation* takes place [11]. The system transits from quasi-periodic motion into periodic one. It is related with the synchronisation effect. On the bifurcation diagrams (Fig. 8) the dark region undergoes a change into two lines, up to $\mu \approx 1.3$. In this point for van der Pol's model the first period doubling bifurcation appears, whereas near $\mu \approx 1.39$ the second period doubling takes place. Next, small

parameter changes lead to the bifurcation cascade and the system transits to the *chaotic region*. The dark area in a range $\mu \in (1.41, 1.57)$ (Fig.8a) corresponds to chaotic vibrations with positive value of the maximal Lyapunov's exponent [13]. At the end of the chaos region, a coexistence of regular and chaotic motion is possible.

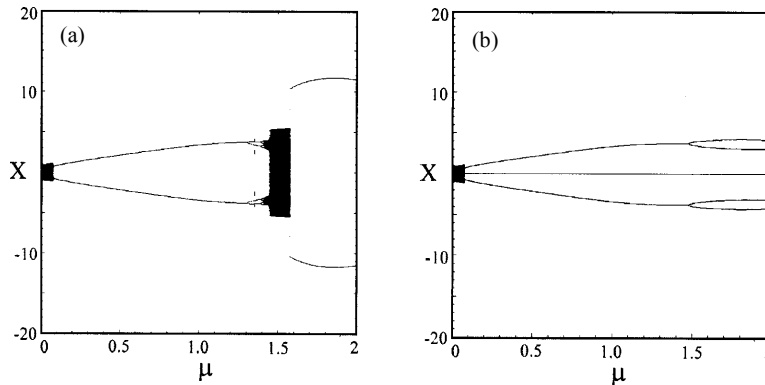


Fig. 8. Bifurcation diagrams versus μ parameter, van der Pol's model (a) , Rayleigh's model (b)

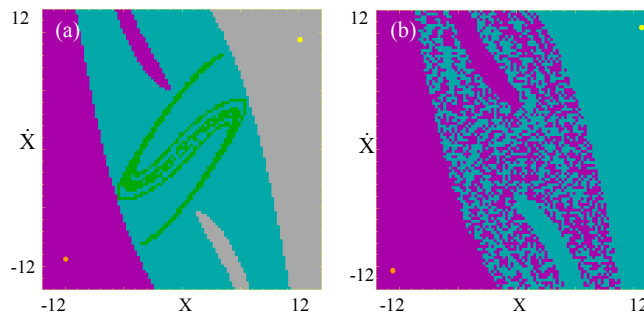


Fig. 9. Evolution of basin of attractions near the chaotic region going out; (a) $\mu=1.55$, (b) $\mu=1.60$

In Fig. 9 the basin of attractions are presented. The bifurcation of *boundary crisis* precedes the going out from chaos to regular motion. The chaotic attractor, visible in the middle of Fig. 9a, is destroyed and only the regular attractor, represented by two points remains.

Rayleigh's damping model does not have such properties. In Fig. 8b after the secondary Hopf's bifurcation the only one period doubling bifurcation is possible and system vibrates periodically. Excited parametrically and Rayleigh's self-excited model does not realize chaotic motion in the tested parameter range.

3. TWO DEGREES OF FREEDOM MODEL

Exemplary calculations of coupled parametrically self-excited oscillators are carried out for two degrees of freedom system presented in Fig. 10. This kind of coupling is often

met in mechanical systems, for instance in gear boxes. Analytical and numerical research confirms, that in the neighbourhood of parametric resonances, the synchronisation phenomenon appears [10] for both damping models. The synchronisation effect is similar to the one degree of freedom model, however it takes place near the first and the second natural frequency neighbourhoods. Nevertheless, the two degree of freedom system, apart from regular and chaotic motion, can generate more complicated vibrations.

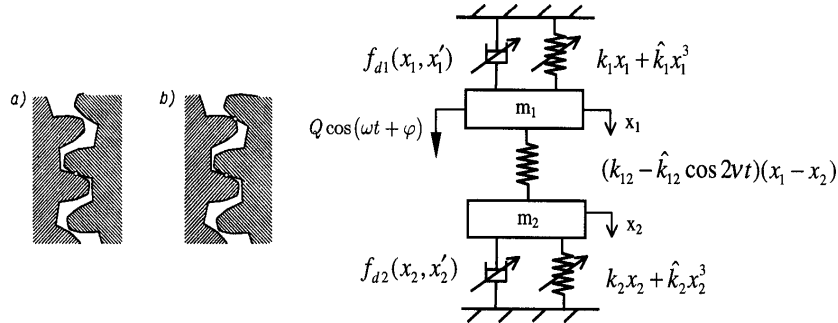


Fig. 10. Model of the parametrically and self-excited system with two degrees of freedom

The motion, which have more than one positive Lyapunov exponent is called hyperchaotic motion [2], [3]. Possible transition of the two coupled parametrically and self-excited Rayleigh's oscillators to hyperchaotic motion is presented in this chapter. The model in Fig. 10 is described by the differential equations of motion

$$\ddot{X}_1 + F_{d1}(X_1, \dot{X}_1) + \delta_1 X_1 + \gamma_1 X_1^3 + (\delta_{12} - \mu \cos 2\vartheta\tau)(X_1 - X_2) = \begin{cases} 0 \\ q \cos \vartheta\tau \end{cases} \quad (17)$$

$$\ddot{X}_2 + MF_{d2}(X_2, \dot{X}_2) + M\delta_2 X_2 + M\gamma_2 X_2^3 - M(\delta_{12} - \mu \cos 2\vartheta\tau)(X_1 - X_2) = 0 \quad (18)$$

where: $F_{d1}(X_1, \dot{X}_1)$, $F_{d2}(X_2, \dot{X}_2)$ are Rayleigh's functions (see chapter 2.1) and dimensionless parameters have values:

$$\alpha_1 = 0.01, \beta_1 = 0.05, \gamma_1 = 3.0, \alpha_2 = 0.01, \beta_2 = 0.05, \gamma_2 = 3.0, \\ M = 0.5, \delta_1 = -0.5, \delta_2 = -0.3, \vartheta = 2.6 \quad (19)$$

It is necessary to underline that the system is strongly non-linear, parameters γ_1 and γ_2 have big values. Furthermore, parameters δ_1 and δ_2 are assumed as negative. It means that linear parts of the springs stiffness are negative [4]. The potential energy graph for assumed parameters (19) is presented in Fig. 11. Selected parameters guarantee that the surface have one maximum and four minimums, *four potential wells*. Numerical simulations of the system with above properties are done taking into account the parametric excitation increase (parameter μ). Two characteristic Poincaré maps for $\mu = 0.5$ and $\mu = 2.0$ are presented in Fig. 12, whereas Lyapunov's exponents values are put in Table 1.

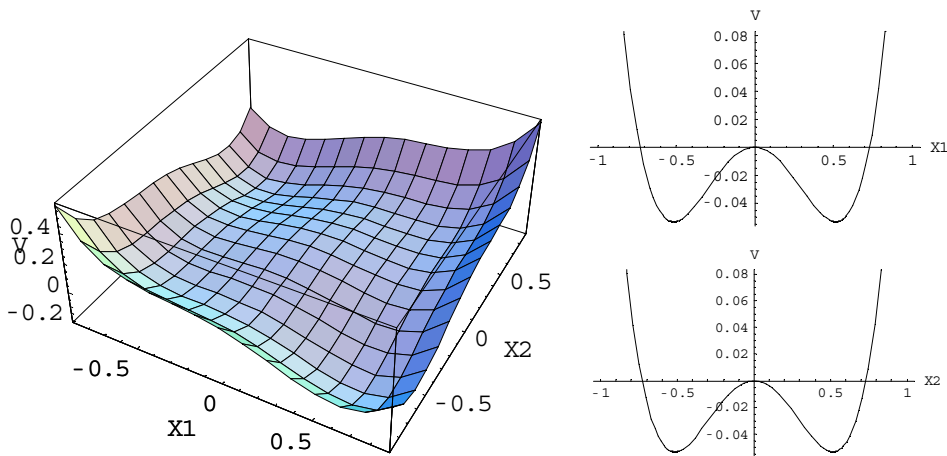


Fig. 11. Potential energy surface and cross sections along X_1 and X_2 axes

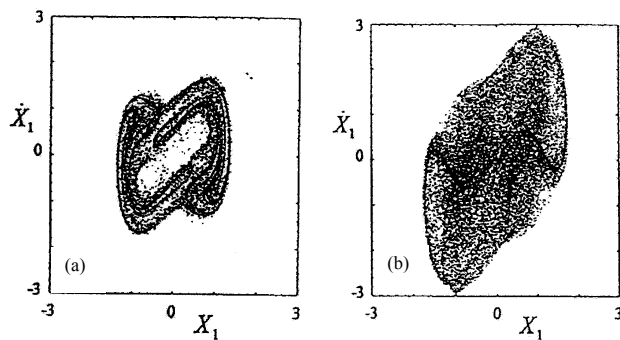


Fig. 12. Poincaré maps for different μ parameters, (a) $\mu=0.5$, (b) $\mu=2.0$

A strange attractor on the Poincaré map (Fig. 12a) obtained for parametric excitation $\mu=0.5$ has a complicated fractal structure with features of chaotic motion. Positive sign of the maximal Lyapunov's exponent in Table 1, for $\mu=0.5$, confirms that the system vibrates chaotically. The attractor in Fig. 12b obtained for $\mu=2.0$ has different character than the former one. Its fractal structure is distinctly complicated. In this case of motion, two Lyapunov's exponents are positive (Table 1). It means that the system vibrates hyperchaotically. This result can be explained by strong parametric and self-excitation interactions and additional influence of the potential energy shape.

Table 1. Lyapunov's exponents

μ	Attractor's type	λ_1	λ_2	λ_3	λ_4	λ_5
0.5	Chaotic	0.144	-0.020	-0.040	-0.244	0.0
2.0	Hyperchaotic	0.162	0.014	-0.152	-0.040	0.0

For the system without four potential wells such an effect does not take place. Thus, the parametrically and self excited system can vibrate periodically inside the synchronisation area, quasi-periodically (the first and the second type quasi-periodic motion, (see [13]), chaotically and furthermore hyperchaotically for the system with four potential wells.

4. SUMMARY AND FINAL CONCLUSIONS

This paper shows new dynamics phenomena resulting from different vibrations type coupling. Interactions between parametric and self-excited vibrations lead to quasi-periodic motion. However, in the neighbourhood of parametric resonances, the system synchronises, and after the inverse secondary Hopf's bifurcation, the motion becomes periodic. Parametric vibrations pull in the self-excitation and the system vibrates with single frequency in the synchronisation areas. The increase of the parametric excitation transmits the system, after the period doubling bifurcation cascade to chaotic motion. For the one degree of freedom system, chaotic motion is possible only for van der Pol's model of self-excitation. During coming out of the chaotic region the coexistence of regular and chaotic attractors is possible. Chaotic attractor is destroyed by the boundary crisis bifurcation.

Important qualitative and quantitative changes in the synchronisation region appears as a consequence of external force introduction. Inside the resonance curve the additional internal loop occurs. This loop is possible only if the external force is not too large. If the external force amplitude q exceeds a limit value, the internal loop disappears and the resonance curve has a typical course.

Additionally, in the system with many degrees of freedom, more complicated motions are possible. Taking the system parameters, giving the potential function with four potential wells, the hyperchaotic motion with two positive Lyapunov exponents is possible. Hyperchaos appears if the parametric excitation is big enough.

It is worth to point out, that if a characteristic of an energy source is taken into account, than the model is called non-ideal. Behaviour of such a system is different comparing with its ideal equivalent model. Vibrations analysis of the non-ideal system with parametric and self-excitation may be found in papers [13] - [16].

REFERENCES

1. Bolotin W.W., (1984), Parametriczeskije rezonansy w avtokolebatielnyh sistemach, *Mechanika tverdogo Tiela*, Nr 5, pp.14-21, (in Russian).
2. Kapitaniak T., Chua L.O., (1994), Hyperchaotic attractors of unidirectionally-coupled Chua's circuits, *International Journal of Bifurcation and Chaos*, 4, pp. 477-482.
3. Kapitaniak T., Steeb W.H.,(1991), Transition to hyperchaos in coupled generalized Van der Pol's equations, *Physics Letters, A* 152, pp. 33-37.
4. Mac Duff J.N., Curren J.R., (1960), *Vibrations in Engineering*, (Levers and negative elasticity coefficients, chapter 9), PWN, Warsaw, (in Polish).
5. Minorski N., (1967), *Mechanical Vibrations*, WNT, Warsaw.
6. Nayfeh A.H., (1981), *Introduction to Perturbation Technique*, J.Wiley, New York.
7. Szabelski K., (1991), The vibrations of self-excited system with parametric excitation and non-symmetric elasticity characteristic, *Journal of Theoretical and Applied Mechanics*, 29, 1, pp.57-81.

8. Szabelski K., Warminski J., (1995), The parametric self excited non-linear system vibrations analysis with the inertial excitation. Int. Journal of Non-Linear Mechanics, Vol.30, No 2, pp.179-189.
9. Szabelski K., Warminski J., (1995), The self excited system vibrations with the parametric and external excitations, Journal of Sound and Vibration, 908, pp. 595-607.
10. Szabelski K., Warminski, J., (1997), Vibrations of a Non-Linear Self-Excited System with Two Degrees of Freedom under External and Parametric Excitation, Journal of Nonlinear Dynamics, 14, pp. 23-36.
11. Thomsen, J.J., (1997), Vibrations and Stability, Order and Chaos, Mc Grow Hill.
12. Tondl A., (1978), On the interaction between self-excited and parametric vibrations, Monographs and Memoranda, No. 25, National Research Institute for Machine Design, Prague.
13. Warminski J., (2001), Regular and Chaotic Vibrations of Parametrically and Self-Excited Systems with Ideal and Non-Ideal Energy Sources, Techn. University of Lublin Publisher, Lublin, p.220, (in Polish).
14. Warminski J., (2001), Synchronisation Effects and Chaos in van der Pol-Mathieu Oscillator, Journal of Theoretical and Applied Mechanics, 4, 39, pp. 861-884.
15. Warminski J., (2002), Regular and Chaotic Vibrations of Van Der Pol-Mathieu Oscillator with Non-Ideal Energy Source, Journal of Theoretical and Applied Mechanics, 2, 40, pp. 415-433.
16. Warminski J., Balthazar J. M., and Brasil R. M. L. R. F., (2001), Vibrations of Non-Ideal Parametrically and Self-Excited Model. Journal of Sound and Vibration, 245 (2), pp. 363-374.
17. Yano S., (1987), Analytic research on dynamic phenomena of parametrically and self excited mechanical systems, Ingenieur-Archiv 57, pp.51-60.

REGULARNE, HAOTIČNE I HIPERHAOTIČNE VIBRACIJE NELINEARNIH SISTEMA SA SAMOPOBUDOM, PARAMETARSKOM I SPOLJAŠNJOM POBUDOM

Jerzy Warminski

Rezultati istraživanja inercija između parametarskih i samopobudnih oscilacija za modela samopobude: van der Pol-ove i Rayleigh-jeve predstavljene su u ovom radu. Pokazano je da u okolini parametarskog rezonantnog režima se javlja fenomen sinhronizacije, kada u tom režimu sistem osciluje kvaziperiodički. Jedna dodatna spoljašnja periodička harmonijska sila je uzrok značajnih promena na rezonantnoj krivoj u okolini glavnog parametarskog opsega. Za dovoljno veliku parametarsku pobudu sistem osciluje slično haotičnom ili hiper haotičnom za model sa četiri potencijalnih "ulegnuća" (minimuma).